Double-diffraction planar encoder by conjugate optics

Ching-Fen Kao
National Chiao Tung University
Institute of Electro-optical Engineering
Hsinchu, Taiwan 30050
and Center for Measurement Standards
Hsinchu, Taiwan 300
E-mail: Alicekao.eo90g@nctu.edu.tw

Calvin C. Chang
Center for Measurement Standards
Hsinchu, Taiwan 300

Mao-Hong Lu, MEMBER SPIE
Institute of Electro-optical Engineering
National Chiao Tung University
Hsinchu, Taiwan 30050

Abstract. A planar encoder using conjugate optics is proposed for sensing the 2-D displacement of a 2-D grating. A Doppler frequency shift of diffracted light is generated when the grating moves. The optical conjugate path can compensate for the error arising from the relative tilt between the optical head and the scale (head-to-scale tilt). Additionally, the optical head is easily integrated, having high tolerance in component-to-component placement. The 2-D displacement system with the 2-D grating, which has period of 1.6 μm in both the X and Y directions, provides a signal period of 0.4 μm by using a double-diffraction configuration. This system and associated electronics provide interpolation with a factor of 400, corresponding to a measurement resolution of 1 nm. [DOI: 10.1117/1.1839227]

Subject terms: displacement sensor; Doppler frequency shift; two-dimensional displacement.

Paper 030629 received Dec. 16, 2003; revised manuscript received May 16, 2004; accepted for publication Jul. 23, 2004; published online Jan. 13, 2005.

1 Introduction

As nanometer-resolution technology has dramatically advanced, studies of biological systems, materials (such as DNA or protein), and manipulative systems have entered the nanometer regime. All of these applications require planar substrate stages for sample scanning. These stages, with high resolution and a long traveling range, generally use heterodyne laser displacement measuring interferometers (DMIs) to locate their positions. DMI sensors provide high resolution in sensing displacement. However, they have the disadvantage of being bulky and expensive, and are difficult to integrate into compact systems. The accuracy of high-performance planar stages depends on the alignment of the workpiece platform with the interferometer's mirrors.

A planar encoder, which comprises a 2-D grating plate and an optical head, is easy to assemble for measuring 2-D displacement.[1] Most recently, several different planar encoders have been designed by using the Moiré[2,3] principle or diffractive principles.[4] Some of these designs, such as those based on the Moiré principle, are of limited resolution. The optical components in many diffraction devices need to be very precisely assembled. A couple of reports on the reading configuration of integrated optical grating scales for sensing one-dimensional displacement have been published.[5,6] Chiang and Lee proposed a rotary or linear encoder based on retroreflection.[7,8] The retroreflection in these encoders provides an interference scheme with equal path lengths. Consequently, interference fringes of high visibility and contrast will be seen.

In this paper, a new design for a 2-D optical encoder with a high head-to-scale tolerance is described. We propose a retroreflection design with optical conjugate path for measuring 2-D displacement. The conjugate configuration can compensate the errors arising from head-to-scale tilt and gives the system high tolerance in component-to-component placement.

2 Theory

2.1 *Configurations and Operational Principles*

As shown in Fig. 1(a), a laser beam is normally incident on a 2-D grating with the same period in both directions. The grating is located in the X-Y plane. The incident plane-wave is $U_{\text{in}}=A_0\exp(-ikz)$, where A_0 is the amplitude of the incident light, and $k=2\pi/\lambda$ is the wave number. The wave vector of the incident light can be written as $\mathbf{k}_{\text{in}}=-k\hat{\mathbf{z}}$, where $\hat{\mathbf{z}}$ is the unit vector in the Z direction. The direction of light diffracted by the 2-D grating can be written as[9,10]

$$\sin\theta=\frac{(v_x^2+v_y^2)^{1/2}}{(v_x^2+v_y^2+v_z^2)^{1/2}}=\frac{[(m/p)^2+(n/p)^2]^{1/2}}{1/\lambda}=\frac{(m^2+n^2)^{1/2}\lambda}{p}. \tag{1}$$

The 2-D grating equation (1) determines the direction of the (m,n) diffraction order for the grating. The diffracted field is denoted by $U_1(m,n)$. The four first diffraction orders, $m=\pm1$ and $n=\pm1$, are considered. Then the diffracted light field U_1, which includes those four orders, can be expressed as

$$U_1=U_1(1,1)+U_1(1,-1)+U_1(-1,1)+U_1(-1,-1), \tag{2a}$$

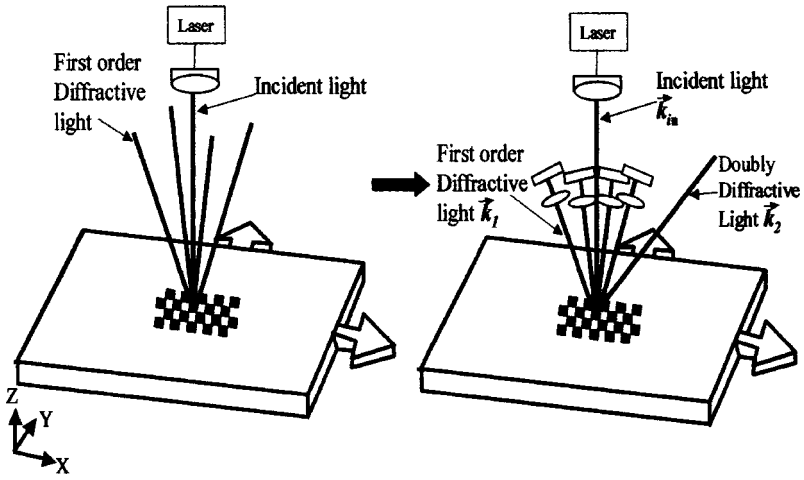

Fig. 1 Diffraction from a 2-D grating. (a) The incident light is diffracted into four first diffraction orders. (b) The four orders are retroreflected by conjugate optics, generating double diffraction.

$$U_1(1,1)=A_1\exp\left(ik_{1,1}z+i2\pi\frac{x+y}{p}\right)$$
$$=A_1\exp(ikz\cos\theta)\exp\left(i\frac{x+y}{\sqrt{2}}k\sin\theta\right), \quad (2b)$$

$$U_1(1,-1)=A_1\exp\left(ik_{1,2}z+i2\pi\frac{x-y}{p}\right)$$
$$=A_1\exp(ikz\cos\theta)\exp\left(i\frac{x-y}{\sqrt{2}}k\sin\theta\right), \quad (2c)$$

$$U_1(-1,1)=A_1\exp\left(ik_{1,3}z-i2\pi\frac{x-y}{p}\right)$$
$$=A_1\exp(ikz\cos\theta)\exp\left(-i\frac{x-y}{\sqrt{2}}k\sin\theta\right), \quad (2d)$$

$$U_1(-1,-1)=A_1\exp\left(ik_{1,4}z-i2\pi\frac{x+y}{p}\right)$$
$$=A_1\exp(ikz\cos\theta)\exp\left(-i\frac{x+y}{\sqrt{2}}k\sin\theta\right), \quad (2e)$$

where A_1 is the amplitude of the first diffraction orders and $\sin\theta=\sqrt{2}\lambda/p$. According to Eq. (1), the four first diffraction orders ($m=\pm1$ and $n=\pm1$) are in the four quadrants of the Cartesian coordinate system. As indicated in Fig. 1(b), these four diffraction orders are retroreflected by conjugate optics and return to the 2-D grating to produce double diffraction. Each set of conjugate optics consists of a collimating lens and a reflective mirror. The mirror is placed on the back focal plane of the lens. For instance, the field $U_1(1,1)$ in Eq. (2) is retroreflected by the conjugate optics and returns to the 2-D grating to produce a doubly diffracted field $U_2(1,1)$, which can be written as

$$U_2(1,1)=U_2(1,1;1,1)+U_2(1,1;1,-1)+U_2(1,1;-1,1)$$
$$+U_2(1,1;-1,-1), \quad (3a)$$

$$U_2(1,1;1,1)=A_2\exp\left[-ik_{1,1;1,1}z\right.$$
$$\left.-i\frac{2\pi(x+y)}{p}\right]\exp\left[i\frac{2\pi(x+y)}{p}\right]$$
$$=A_2\exp(ikz), \quad (3b)$$

$$U_2(1,1;1,-1)=A_2\exp\left[-ik_{1,1;1,-1}z\right.$$
$$\left.-i\frac{2\pi(x+y)}{p}\right]\exp\left[i\frac{2\pi(x-y)}{p}\right]$$
$$=A_2\exp[-i\sqrt{2}ky\sin\theta+ikz(\cos2\theta)^{1/2}], \quad (3c)$$

$$U_2(1,1;-1,1)=A_2\exp\left[-ik_{1,1;-1,1}z-i\frac{2\pi(x+y)}{p}\right]$$
$$\times\exp\left[-i\frac{2\pi(x-y)}{p}\right]$$
$$=A_2\exp[-i\sqrt{2}kx\sin\theta+ikz(\cos2\theta)^{1/2}], \quad (3d)$$

$$U_2(1,1;-1,-1)=A_2\exp\left[-ik_{1,1;-1,-1}z\right.$$
$$\left.-i\frac{2\pi(x+y)}{p}\right]\exp\left[-i\frac{2\pi(x+y)}{p}\right]$$
$$=A_2\exp[-i\sqrt{2}k(x+y)\sin\theta+ikz(1$$
$$-4\sin^2\theta)^{1/2}]. \quad (3e)$$

The double diffraction is denoted by $(m,n;m',n')$, where (m',n') represents the order of the double diffraction and (m,n) represents the order of the original diffraction that produces it. Similarly, the field $U_1(1,-1)$ in Eq. (2) is retroreflected by the other conjugate optics and returns to the 2-D grating to produce the field $U_2(1,-1)$ of the double diffraction, which can be written as

$$U_2(1,-1)=U_2(1,-1;1,1)+U_2(1,-1;1,-1)+U_2(1,-1;-1,1)+U_2(1,-1;-1,-1), \tag{4a}$$

$$U_2(1,-1;1,1)=A_2\exp[i\sqrt{2}ky\sin\theta+ikz(\cos 2\theta)^{1/2}], \tag{4b}$$

$$U_2(1,-1;1,-1)=A_2\exp(ikz), \tag{4c}$$

$$U_2(1,-1;-1,1)=A_2\exp[-i\sqrt{2}k(x-y)\sin\theta+ikz(1-4\sin^2\theta)^{1/2}], \tag{4d}$$

$$U_2(1,-1;-1,-1)=A_2\exp[-i\sqrt{2}kx\sin\theta+ikz(\cos 2\theta)^{1/2}]. \tag{4e}$$

Next, we consider the change of angular frequency in the interference caused by the Doppler effect[11,12] when the 2-D grating moves. In Fig. 1(b), we denote the wave vector of the first diffracted field $U_1(1,1)$ by $\mathbf{k}_1$, the wave vector of the double diffraction $U_2(1,1;-1,1)$ by $\mathbf{k}_2$, and the wave vector of the incident light by $\mathbf{k}_{\text{in}}$. According to Eq. (3), the wave vector of the light can be expressed as

$$\mathbf{k}_{\text{in}}=-k\hat{\mathbf{z}},$$

$$\mathbf{k}_1=\frac{1}{\sqrt{2}}k\sin\theta\,\hat{\mathbf{x}}+\frac{1}{\sqrt{2}}k\sin\theta\hat{\mathbf{y}}+k\cos\theta\,\hat{\mathbf{z}}, \tag{5}$$

$$\mathbf{k}_2=-\sqrt{2}k\sin\theta\,\hat{\mathbf{x}}+k(\cos 2\theta)^{1/2}\hat{\mathbf{z}}.$$

The change of the angular frequency is given by

$$\Delta\omega_1=(\mathbf{k}_1-\mathbf{k}_{\text{in}})\cdot\mathbf{V}_g+(\mathbf{k}_2+\mathbf{k}_1)\cdot\mathbf{V}_g, \tag{6}$$

where $\mathbf{V}_g$ is the velocity of the 2-D grating and is written as $\mathbf{V}_g=V_{gx}\hat{\mathbf{x}}+V_{gy}\hat{\mathbf{y}}$. From Eq. (6), we have

$$\Delta\omega_1=\left(\frac{1}{\sqrt{2}}k\sin\theta\,\hat{\mathbf{x}}+\frac{1}{\sqrt{2}}k\sin\theta\,\hat{\mathbf{y}}+k\cos\theta\,\hat{\mathbf{z}}+k\hat{\mathbf{z}}\right)\cdot(V_{gx}\hat{\mathbf{x}}+V_{gy}\hat{\mathbf{y}})+\left[-\sqrt{2}k\sin\theta\,\hat{\mathbf{x}}+k(\cos 2\theta)^{1/2}\hat{\mathbf{z}}+\frac{1}{\sqrt{2}}k\sin\theta\,\hat{\mathbf{x}}+\frac{1}{\sqrt{2}}k\sin\theta\,\hat{\mathbf{y}}+k\cos\theta\,\hat{\mathbf{z}}\right]\cdot(V_{gx}\hat{\mathbf{x}}+V_{gy}\hat{\mathbf{y}})=\sqrt{2}k\sin\theta\,V_{gy}. \tag{7}$$

Similarly, in Fig. 1(b), we denote the wave vector of the first diffracted field $U_1(1,-1)$ by $\mathbf{k}_1$, the wave vector of the doubly diffracted field $U_2(1,-1;-1,-1)$ by $\mathbf{k}_2$, and the wave vector of the incident light by $\mathbf{k}_{\text{in}}$. According to Eq. (4), the wave vector of the light can be expressed as

$$\mathbf{k}_{\text{in}}=-k\hat{\mathbf{z}},$$

$$\mathbf{k}_1'=\frac{1}{\sqrt{2}}k\sin\theta\,\hat{\mathbf{x}}-\frac{1}{\sqrt{2}}k\sin\theta\,\hat{\mathbf{y}}+k\cos\theta\,\hat{\mathbf{z}}, \tag{8}$$

$$\mathbf{k}_2=-\sqrt{2}k\sin\theta\,\hat{\mathbf{x}}+k(\cos 2\theta)^{1/2}\hat{\mathbf{z}}.$$

The change of the angular frequency can be described as

$$\Delta\omega_2=-\sqrt{2}k\sin\theta\,V_{gy}. \tag{9}$$

The doubly diffracted fields $U_2(1,1;-1,1)$ and $U_2(1,-1;-1,-1)$ propagate in the same direction, so the amplitude distributions can be expressed as

$$E_1=A_2\exp\{i[(w+\Delta w_1)t+\phi_0]\}, \tag{10}$$

$$E_2=A_2\exp\{i[(w+\Delta w_2)t+\phi_0]\}. \tag{11}$$

The light intensity I_y of the superposition of the two beams is given by[13]

$$\begin{aligned}I_y\propto|E_1+E_2|^2&=|A_2|^2[2+2\cos(\Delta w_2-\Delta w_1)t]\\&=|A_2|^2[2+2\cos(2\sqrt{2}V_{gy}k\sin\theta\,t)]\\&=|A_2|^2[2+2\cos(2\sqrt{2}k\sin\theta\,\Delta y)]\\&=|A_2|^2\left[2+2\cos\left(\frac{8\pi\Delta y}{p}\right)\right],\end{aligned} \tag{12a}$$

where Δy is the displacement in the Y direction. Likewise, the light intensity of interference due to the displacement in the X direction can be expressed as

$$I_x=|A_2|^2\left[2+2\cos\left(\frac{8\pi\Delta x}{p}\right)\right], \tag{12b}$$

where Δx is the grating displacement in the X direction. As mentioned, the 2-D displacement can then be obtained.

2.2 *Head-to-Scale Tolerance*

When the planar encoder is applied in a position control system, such as a planar motor, any wobble can cause some tilt between the encoder head and the scale grating. As shown in Fig. 2, the scale grating lies on the X-Y plane. The angle between the incident light and the normal to the grating is $\Delta\eta$, and the azimuth angle is $\Delta\xi$. If this tilt condition is considered, the wave vectors of the incident light and diffracted beams in Eq. (5) become

$$\mathbf{k}_{\text{in}}=-(k\sin\Delta\eta\cos\Delta\xi)\hat{\mathbf{x}}-(k\sin\Delta\eta\sin\Delta\xi)\hat{\mathbf{y}}-(k\cos\Delta\eta)\hat{\mathbf{z}},$$

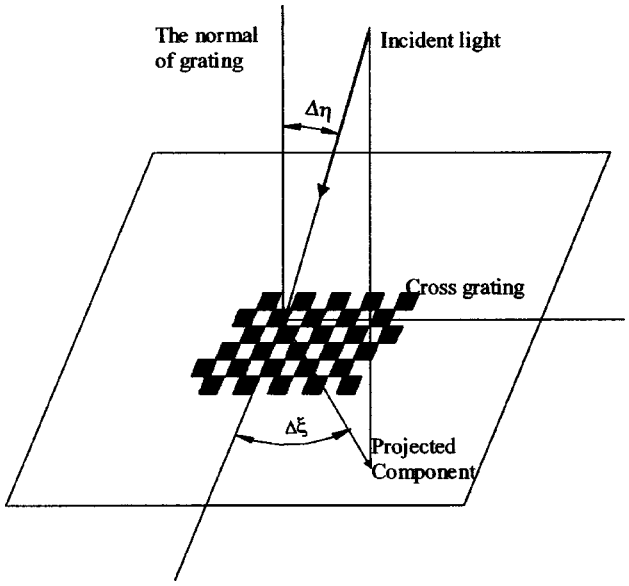

Fig. 2 Tilt between incident beam and 2-D grating. The angle between the incident light and the normal to the grating is $\Delta\eta$. The azimuth angle is $\Delta\xi$.

$$\mathbf{k}_1 = k\left(-\sin\Delta\eta\cos\Delta\xi + \frac{1}{\sqrt{2}}\sin\theta\right)\hat{\mathbf{x}} + k\left(-\sin\Delta\eta\sin\Delta\xi + \frac{1}{\sqrt{2}}\sin\theta\right)\hat{\mathbf{y}} + k_{1Z}\hat{\mathbf{z}}, \tag{13}$$

$$\mathbf{k}_2 = k(\sin\Delta\eta\cos\Delta\xi - \sqrt{2}\sin\theta)\hat{\mathbf{x}} + k_{2Z}\hat{\mathbf{z}}.$$

The change of angular frequency from the Doppler effect can be rewritten as

$$\begin{aligned}\Delta\omega_1 &= (\mathbf{k}_1 - \mathbf{k}_{\text{in}})\cdot\mathbf{V}_g + (\mathbf{k}_2 + \mathbf{k}_1)\cdot\mathbf{V}_g \\ &= \left(\frac{1}{\sqrt{2}}k\sin\theta\,\hat{\mathbf{x}} + \frac{1}{\sqrt{2}}k\sin\theta\,\hat{\mathbf{y}} + k\cos\theta\,\hat{\mathbf{z}} - k\hat{\mathbf{z}}\right)\cdot(V_{gx}\hat{\mathbf{x}} + V_{gy}\hat{\mathbf{y}}) \\ &\quad + \left[-\sqrt{2}k\sin\theta\,\hat{\mathbf{x}} + k(\cos 2\theta)^{1/2}\hat{\mathbf{z}} + \frac{1}{\sqrt{2}}k\sin\theta\,\hat{x} + \frac{1}{\sqrt{2}}k\sin\theta\,\hat{y} + k\cos\theta\,\hat{z}\right]\cdot(V_{gx}\hat{x} + V_{gy}\hat{y}) \\ &= \sqrt{2}k\sin\theta\,V_{gy}.\end{aligned} \tag{14}$$

Similarly, Eq. (8) becomes

$$\mathbf{k}_{\text{in}} = -k(\sin\Delta\eta\cos\Delta\xi)\hat{\mathbf{x}} - k(\sin\Delta\eta\sin\Delta\xi)\hat{\mathbf{y}} - k(\cos\Delta\eta)\hat{\mathbf{z}},$$

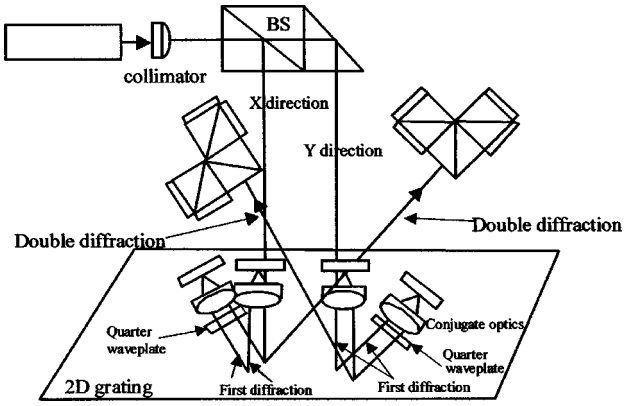

Fig. 3 Scheme of experimental setup for planar encoder. A He-Ne laser is the light source, and a beamsplitter cube divides the light into two beams for *X*- and *Y*-direction measurements.

$$\mathbf{k}_1' = k\left(-\sin\Delta\eta\cos\Delta\xi + \frac{1}{\sqrt{2}}\sin\theta\right)\hat{\mathbf{x}} + k\left(-\sin\Delta\eta\sin\Delta\xi - \frac{1}{\sqrt{2}}\sin\theta\right)\hat{\mathbf{y}} + k_{1Z}\hat{\mathbf{z}}, \tag{15}$$

$$\mathbf{k}_2 = k(\sin\Delta\eta\cos\Delta\xi - \sqrt{2}\sin\theta)\hat{\mathbf{x}} + k_{2Z}\hat{\mathbf{z}}.$$

The change of angular frequency is

$$\Delta\omega_2 = -\sqrt{2}k\sin\theta\,V_{gy}. \tag{16}$$

Equations (13) and (15) imply that the two doubly diffracted beams propagate in the same direction when the wobble causes a tilt between the encoder head and the scale grating. From Eqs. (14) and (16), such a tilt does not affect the changes $\Delta\omega_1$ and $\Delta\omega_2$ of the angular frequency. Therefore, the tilt can be automatically compensated without any effect on the measurement of displacement in this configuration. However, the size of the optical components does affect the head-to-scale tolerance.

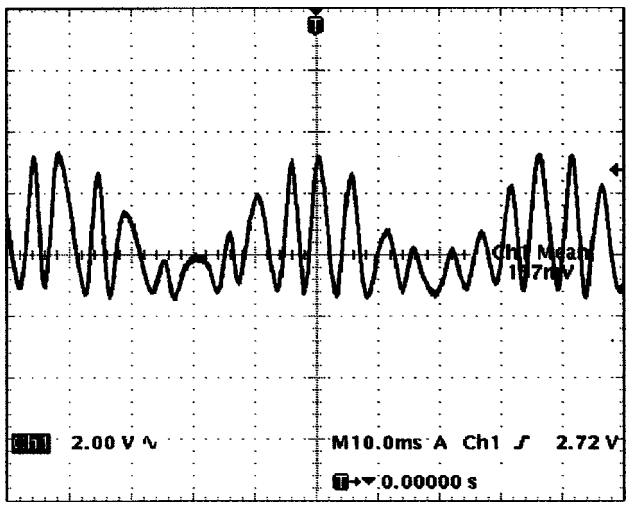

Fig. 4 Enveloping sinusoidal signal formed by three interferences.

3 Experiment

3.1 *Experimental Setup*

Figure 3 shows the experimental setup. A 2-D grating with a period of 1.6 μm, a depth of 150 nm, and a duty ratio of 0.5 was used. When a He-Ne laser beam with fiber guiding was incident on the grating, several diffracted beams were generated (as shown in Fig. 1), including, for example, the first orders (1,1), (1,−1), (−1,1), (−1,−1), the second orders (0,2), (2,0), and so on. As mentioned in Sec. 2.2, the four first-order diffracted beams were retroreflected by the optical conjugate system and generated double diffractions. The double diffractions (1,−1;−1,−1) and (1,1;−1,1) were very close to the original second-order (−2,0) diffracted beam, and would yield an extra undesired interference, as shown in Fig. 4. In order to avoid such interference, we resorted to shifted optics that separates the original second-order diffracted beam from the doubly diffracted beams, and avoids interference between the doubly diffracted beam and the original second-order diffractions, as shown in Fig. 5. Therefore, only a pure sinusoidal signal of the interference between the double diffractions was left.

Let us consider the first diffraction orders (1,1) and (1,−1), which are retroreflected by conjugate optics. The conjugate optics comprises a doublet lens with focal length 8 mm and a planar mirror. The light reflected by the mirror is incident again on the 2-D grating, which generates double diffractions (1,−1;−1,−1) and (1,1;−1,1) in the same direction. Then these double diffractions (1,−1;−1,−1) and (1,1;−1,1) interfere with each other. A piezotransducer planar stage was used to move the 2-D grating. Figure 6 shows the generated sinusoidal signals when the stage moved along AB and BC in a hexagonal path. The solid sinusoidal curve represents the Y-axis displacement, and the dashed sinusoidal curve represents the X-axis displacement.

For measurement purposes, the two orthogonal sinusoidal signals (sine and cosine) are produced by phase-shift signals with a polarization and retarder plate.[14] As shown in Fig. 3, a quarter-wave plate is inserted into one path of the conjugate optics. The quarter-wave plate is inserted into the path of the first diffraction order (1,−1), and the (1,−1) beam is retroreflected by the conjugate optics. Therefore, the (1,−1) beam passes twice through the quarter-wave plate. The first diffraction orders (1,1) and (1,−1) are reflected by the grating and induce two doubly diffracted beams with orthogonal polarizations.

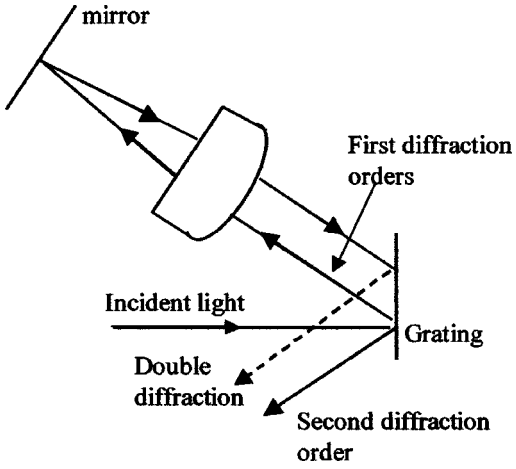

Fig. 5 Conjugate optics with shifted optical axes.

As shown in Fig. 7(a), the double diffraction, which propagates along the Z axis, is divided into four beams by beamsplitters. Polarizers are inserted into the paths of the four beams with different azimuths. The phase variation of the light that penetrates the polarizer located with a specific azimuth in the path of the circularly polarized beam can be calculated with the Jones calculus. For example, as shown in Fig. 7(b), the doubly diffracted beam is perpendicular to polarizer 3, which has an azimuth of 0 (horizontally polarized). The intensity I_1 of the interference between the horizontal components of the two doubly diffracted beams is given by

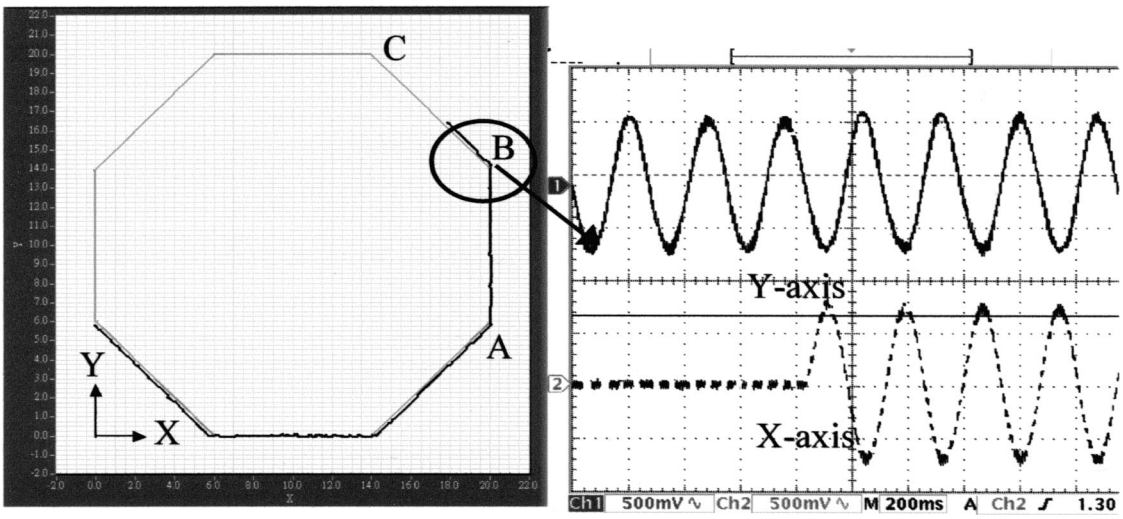

Fig. 6 Sinusoidal signals as the stage moves along AB and BC in a hexagonal path.

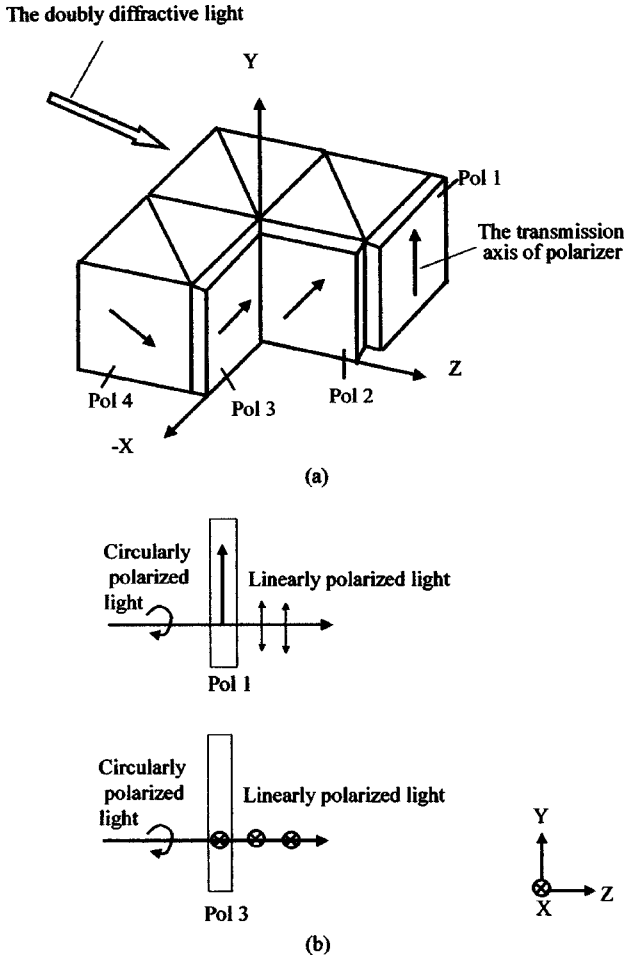

Fig. 7 (a) Scheme for phase-shift module. (b) The horizontal and vertical components of the doubly diffracted beams.

$$I_1=|E''_{1x}+E''_{2x}|^2=\left|\frac{E''_0 e^{i\phi}}{\sqrt{2}}\begin{bmatrix}1\\0\end{bmatrix}+\frac{iE''_0}{\sqrt{2}}\begin{bmatrix}1\\0\end{bmatrix}\right|^2$$

$$=\frac{E''^2_0}{2}\left|\begin{bmatrix}e^{i\phi}+\exp(i\pi/2)\\0\end{bmatrix}\right|^2=\frac{E''^2_0}{2}\left[2+2\cos\left(\phi-\frac{\pi}{2}\right)\right]. \tag{17}$$

Similarly, the doubly diffracted beams pass through polarizer 1 with an azimuth of 90 deg (vertically polarized). The intensity I_2 of the interference between the vertical components of the two doubly diffracted beams, and the interference intensities I_3 for the $+45$-deg component and I_4 for the -45-deg component, can be expressed as

$$I_2=\frac{E''^2_0}{2}\left[2+2\cos\left(\phi+\frac{\pi}{2}\right)\right],$$

$$I_3=\frac{E''^2_0}{2}(2+2\cos\phi), \tag{18}$$

$$I_4=\frac{E''^2_0}{2}[2+2\cos(\phi+\pi)].$$

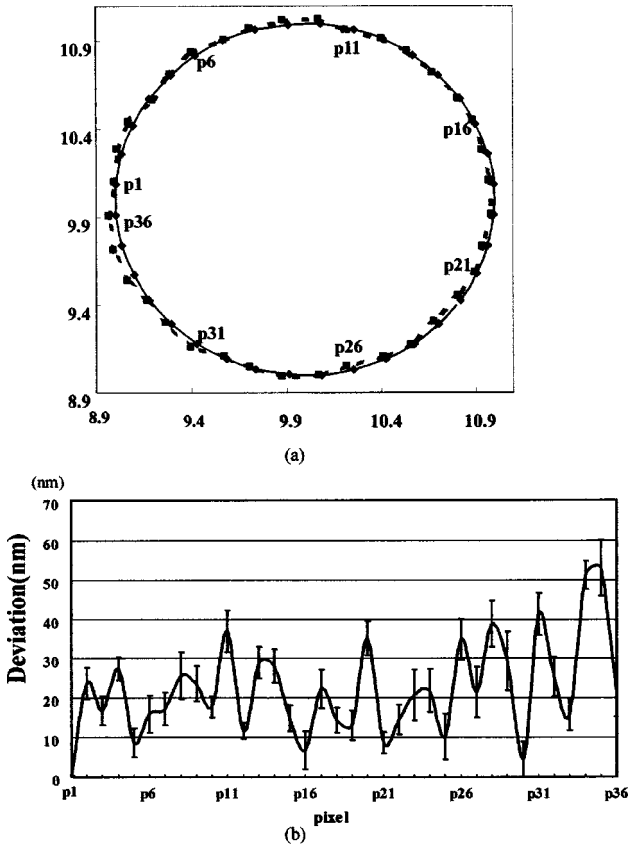

Fig. 8 (a) Circles measured by the capacitance displacement sensor (solid) and the planar encoder (dotted). (b) The differences between the measurements and the standard deviation of the repeatability measurements.

From these equations, four signals are obtained, which have phase shifts of 90 deg with respect to each other. The encoder head gives a signal period of 0.4 μm, which is one-quarter of the scale pitch 1.6 μm. An electronic interpolation by using the IK220[15] (Heidenhain Inc.) with an interpolation factor of 400 gives a measurement resolution of 1 nm.

3.2 *Results and Discussion*

A piezo positioning system from PI Inc. with a scanning range of 20 μm was used to measure the accuracy of the planar encoder. A flexure stage with a high mechanical stiffness and excellent guidance accuracy provides nanometer resolution, linearity of 0.1%, and repeatability of ± 5 nm by means of an internal capacitance displacement sensor. We measured a circle with radius 10 μm. In the Fig. 8(a), the dotted circle was measured by the encoder, and the solid circle by the capacitive sensor. The readings of the encoder and sensor are denoted by (x_e, y_e) and (x_c, y_c), respectively. The difference between the two measurements, $[(x_e-x_c)^2+(y_e-y_c)^2]^{1/2}$, is plotted in Fig. 8(b), where the horizontal axis gives the pixel number for the pixels sampling the circle. The maximum difference between the measured values is 51 nm. This difference includes the intrinsic periodic error of the 2-D gratings, an inherent nonlinearity of this positioning system, and noise of the electronic circuit. As shown in Fig. 8(b), the circle

was measured 10 times to check the repeatability of the encoder. The standard deviation of the repeatability measurements is better than 7 nm.

In this experiment, the aperture of the conjugate optics is 3.5 mm, the diameter of the incident beam is 1 mm, the aperture of the detector is 3 mm, and the distance between the grating and the conjugate optics is 8 mm. The tolerance region of the incident beam is about 1.5 mm. The head-to-scale tolerance can be calculated as

$$\Delta\eta = \pm \sin^{-1}(0.75/8) = \pm 5.4 \text{ deg.} \tag{19}$$

4 Conclusions

A planar encoder with a high head-to-scale tolerance has been developed. In this encoder, conjugate optics has been used, which has two advantages. First, the double diffraction gives a signal period 0.4 μm, which is only one-quarter of the scale period (1.6 μm). An electronic interpolation with a factor of 400 leads to a measurement resolution of 1 nm. Second, the head-to-scale relation does not affect the interference between the diffractive beams and consequently gives a large tolerance for the measuring system. The uniformity of the grating pitch, the diffractive efficiency of the grating, and the interpolation error (which depends on the dc offset, the amplitudes of the sinusoidal signals, and the phase difference between those signals) all affect the performance of the planar encoder. This equal-path configuration can provide almost 100% fringe contrast. Therefore, we can use a low-coherence light source, such as a diode laser. Further efforts can be directed toward improving the diffractive efficiency of the cross grating and integrating the conjugate optics module with the detection module and the laser source module.

Acknowledgments

This work was supported by the Ministry of Economic Affairs of the Republic of China, Taiwan, under contract No. MOEA 91-EC-2-A-17-0337.

References

1. M. L. Schattenburg and H. I. Smith, ''The critical role of metrology in nanotechnology,'' in *Workshop on Nanostructure Science, Metrology and Technology, Proc. SPIE* **4608**, 1–8 (2001).
2. D. Crespo, T. Morlanes, and E. Bernabeu, ''Optical encoder based on the Lau effect,'' *Opt. Eng.* **39**, 817–824 (2000).
3. D. Crespo, J. Alonso, and E. Bernabeu, ''Reflection optical encoders as three-grating moire systems,'' *Appl. Opt.* **39**, 3805–3813 (2000).
4. J.-D. Lin and H.-B. Kuo, ''Development of a new optical scale system by the diffractive phase interference method,'' *Meas. Sci. Technol.* **6**, 293–296 (1995).
5. B. Geh and A. Dorsel, ''Integrated optical grating scale readout employing a double grating,'' *Appl. Opt.* **31**, 5241–5245 (1992).
6. S. Ura, M. Shinohara, T. Suhara, and H. Nishihara, ''Integrated-optic grating-scale-displacement sensor using linearly focusing grating couplers,'' *IEEE Photonics Technol. Lett.* **6**, 239–241 (1994).
7. W.-W. Chiang and C. K. Lee, ''Wavefront reconstruction optics for use in a disk drive position measurement system,'' U.S. Patent No. 5,442,172 (1995).
8. C. C. Wu, Y. C. Chen, C. K. Lee, C. T. Hsieh, W. J. Wu, and S. S. Lu, ''Design verification of a linear laser encoder with high head-to-scale tolerance,'' *Proc. SPIE* **3779**, 73–82 (1999).
9. J. W. Goodman, *Introduction to Fourier Optics*, McGraw-Hill (1968).
10. H. J. Caulfield, *Handbook of Optical Holography*, Chap. 2, pp. 40–43, Academic Press (1979).
11. M. G. Moharam and T. K. Gaylord, ''Analysis and applications of optical diffraction by gratings,'' *Proc. IEEE* **73**, 894–937 (1985).
12. M. Bass and E. W. Van Stryland, *Handbook of Optics*, Vol. 2, Chap. 30, p. 18, McGraw-Hill (1994).
13. W. J. Wu, C. K. Lee, and C. T. Hsieh, ''Signal processing algorithms for Doppler effect based nanometer positioning,'' *Jpn. J. Appl. Phys., Part 1* **38**, 1725–1729 (1999).
14. C. L. Koliopoulos, ''Simultaneous phase shift interferometer,'' *Proc. SPIE* **1531**, 119–127 (1991).
15. *IK220 PC Counter Card User's Manual*, Heidenhain Corp. (Mar. 2002).

Ching-Fen Kao graduated from Chun-Yuan Christian University, Taiwan, in 1987, and received the MS degree in optical engineering from National Central University, Taiwan, in 1989. Since 1991, she has been with the Precision Instrument Development Center of the National Science Council and the Center for Measurement Standards at the Industrial Technology Research Institute in Taiwan. She is currently a candidate for the doctor's degree at the Institute of Electro-optical Engineering, National Chiao-Tung University, where her research mainly concerns the development of position sensors and precision dimensional metrology.

Calvin C. Chang received his MS degree in mechanical engineering in 1989 from the University of Cincinnati, Ohio, and his PhD in engineering mechanics in 1993 from the University of Texas at Austin. He is currently a senior engineer at the Center for Measurement Standards, Industrial Technology Research Institute, in Taiwan. His research primarily concerns precision dimensional metrology in the field of micro- to nanotechnology.

Mao-Hong Lu graduated from the Department of Physics at Fudan University in 1962. He then worked as a research staff member at the Shanghai Institute of Physics and Technology, Chinese Academy of Sciences, from 1962 to 1970, and the Shanghai Institute of Laser Technology from 1970 to 1980. He studied at the University of Arizona as a visiting scholar from 1980 to 1982. He is currently a professor at the Institute of Electro-optical Engineering, National Chiao-Tung University.